JOURNAL OF NEUROPHYSIOLOGY
Vol. 73, No. 4, April 1995. *Printed in U.S.A.*

Emergence of Complex Receptive Field Properties of Ganglion Cells in the Developing Turtle Retina

EVELYNE SERNAGOR AND NORBERTO M. GRZYWACZ
The Smith-Kettlewell Eye Research Institute, San Francisco, California 94115

SUMMARY AND CONCLUSIONS

1. Receptive field properties of adult retinal ganglion cells are well documented, but little is known about their development. We made extracellular recordings of activity from turtle retinal ganglion cells during embryogenesis (stages 22–26), during the first 40 days posthatching, and in adults.

2. From stage 22 the cells fired in spontaneous recurring bursts, and from stage 23 they responded to light. Polar plots of the responses to motion were highly anisotropic in early embryonic cells. More than 40% of embryonic cells exhibited multiaxis anisotropy, and only 6% were statistically isotropic. The incidence of anisotropic cells gradually decreased throughout development. The incidence of isotropic cells and the excitatory receptive field diameters of all ganglion cells gradually increased during development and their maturation coincided with the disappearance of the spontaneous bursts (2–4 wk posthatching).

3. Both sensitivities to stimulus orientation and direction of motion were observed at the earliest stages of development. However, orientation selectivity reached a peak incidence at hatching, whereas directional selectivity completely disappeared, only to reappear in adults.

4. These results show that mature spatiotemporal receptive field properties of retinal ganglion cells emerge from initially highly anisotropic properties, which may reflect an immature, polarized dendritic layout. Their maturation might be mediated by dendritic outgrowth and strengthening of excitatory synaptic connections, which could be induced by spontaneous activity and driven to maturation by exposure to light at birth. Mature directional selectivity seems to require visual experience or the late establishment of a specialized inhibitory synaptic drive.

INTRODUCTION

Retinas of small-brained vertebrates exhibit complex receptive field properties such as sensitivities for direction of motion and stimulus orientation. Such properties are well documented in adult retinas (Amthor and Grzywacz 1993; Marchiafava 1979; Maturana et al. 1960). However, little is known about how these properties are shaped during embryogenesis and neonatal life (Dacheux and Miller 1981a,b; Masland 1977) and which factors affect their maturation (Daw and Wyatt 1974). Studying the development of these properties and retinal morphological features may help to elucidate cellular mechanisms underlying the function of the mature retina itself.

Detailed anatomic studies of developing ganglion cells in mammals (Dunlop 1990; Maslim et al. 1986; Ramoa et al. 1988) and avians (Vanselow et al. 1990) show that immature ganglion cells have small polarized dendritic trees and that the dendrites expand, branch, and stratify with maturation. Immature mammalian ganglion cells fire spontaneously in recurring bursts of action potentials that are synchronized between neighboring cells (Maffei and Galli-Resta 1990), resulting in propagating excitatory waves across the retina (Meister et al. 1991; Wong et al. 1993). This spontaneous activity disappears at some time after birth. Rabbit ganglion cells first respond to light 6 days after birth, at the same time that synapses in both the outer and inner plexiform layers become functional (Dacheux and Miller 1981a,b; Masland 1977). Receptive field properties of rabbit ganglion cells such as surround inhibition, concentric fields, or directional selectivity can be seen when these cells start responding to light. The incidence of directional selectivity increases and plateaus during the 2nd and 3rd postnatal wk (Masland 1977), coinciding with an increase of synaptic density in the inner plexiform layer.

The turtle retina provides the ideal preparation for developmental studies of light responses of ganglion cells because these cells start responding to light early during embryogenesis and their development is slow. In general, neural functions mature much earlier in oviparous species than in mammals because oviparous animals must be independent as soon as they hatch to survive and escape predators, whereas mammals rely on maternal protection. Sea turtles, for instance, use visual cues to find their way to the ocean as soon as they hatch on the beach (Lohmann 1992). With this information in mind, it becomes obvious that the retina must be prepared for sensory stimulation during embryogenesis to be fully functional as soon as hatching occurs.

Here we are able to describe for the first time how spatiotemporal receptive field properties of turtle ganglion cells are shaped from early embryonic stages on. Part of this study has already been published in abstract form (Sernagor and Grzywacz 1993, 1994) and has been briefly summarized (Grzywacz et al. 1995).

METHODS

We used the turtle species *Pseudemys Scripta Elegans.* The age of the embryos was determined according to specific stages of embryonic development (Yntema 1968) rather than according to the absolute embryonic age. Adult turtles were chosen according to their carapace length of 10–15 cm. After ≥8 h of dark adaptation the turtles (at all ages) were quickly decapitated and pithed under infrared illumination while viewed with an infrared monocular viewer (model 6100M, Electrophysics, Nutley, NJ) (Borg-Graham and Grzywacz 1990). The following steps of the dissection were performed under infrared microscopy (Javelin JE-7242, Los Angeles, CA). After enucleation, the eye was hemisected with fine scissors while submerged in Ringer solution. The composition of the Ringer solution was the following (in mM): 96.5 NaCl, 2.6

KCl, 2.0 $MgCl_2$, 31.5 Na_2CO_3, 10 glucose, 10 *N*-2-hydroxyethylpiperazine-*N'*-2-ethanesulfonic acid, and 4 $CaCl_2$, pH 7.4 (when oxygenated). The adult eyecup was cut in two to three pieces that did not include the optic disc. Pieces that clearly included the visual streak were chosen for isolation. Almost the entire retina (excluding the optic disc) was removed in one piece in embryos and hatchlings (the entire eye has a diameter of 2–3 mm). The streak was not visible at these stages. After selecting a piece for isolation, we gently peeled the retina off the sclera with a pair of fine forceps. The isolated retinal piece was then laid, ganglion cells facing down, on a small piece of nitrocellulose filter paper (0.45 μm) with a 1- to 1.5-mm window and gently flattened around the window. For immature retinas, the central part of the retina was centered above the window to ensure recording from central rather than peripheral retina. The retina was then placed (photoreceptor down) in the experimental chamber on the stage of a Zeiss Axioscope microscope (with fixed stage) fitted with an infrared camera (Hamamatsu C2400). The preparation was superfused at a rate of 4–10 ml/s with oxygenated Ringer solution kept at 26–28°C. The microscope's condenser focused the stimuli from a Tektronix 608 monitor (controlled by a Picasso waveform generator, Innisfree, Cambridge, UK) onto the retina (maximal retinal illumination $\approx$120 lx). Extracellular electrodes (parylene coated, 5 MΩ, A-M Electrophysiology) accessed the ganglion cells through the filter paper window. An IBM PC compatible computer running ASYST 2.1 (ASYST, Rochester, NY) recorded and analyzed the data and controlled the stimuli.

The receptive field diameter was measured with a 9 × 9 array of 100 × 100 μm^2 nonoverlapping squares of light covering a 900 × 900 μm^2 area on the retina. Squares appeared in random order and each square was illuminated (turned on and off) 10 times over 12 continuous seconds. Therefore the duration of the illumination cycle was 1.2 s (0.6 s on and 0.6 s off). The response for each receptive field position was defined as the total number of spikes elicited over the 12 s of sampling. On some occasions, light-driven responses were contaminated by spontaneously occurring bursts. It was not possible to isolate the light-evoked spikes from the overall activity by temporally correlating the pattern of discharge with the onset and offset of the light stimulus. The reason was that spontaneous bursts can be extremely prolonged (several seconds) and irregular in their duration and frequency of occurrence. To eliminate contamination from spontaneous bursts, we tested for each position whether the average number of spikes in trials 2 to 5 was statistically different from the number of spikes in trials 6 to 10 (2-sided *t*-test, $P < 0.01$, 7 degrees of freedom). We removed trial 1 from this statistical test because it may have contained transient responses. [The trial duration of 1.2 s was longer than the duration of light-adaptation transients in adult retinas, and thus probably longer than transients in developing retinas, which fatigue more rapidly (Dacheux and Miller 1981b).] If a difference existed, we substituted the mean response from (noncontaminated) neighbor positions for the contaminated data. After removal of burst contamination, we normalized the array containing the spike count for each square such that the sum of entries became unity and thus the array became a probability distribution. From the normalized array we calculated the horizontal and vertical positional standard deviations and set the receptive field diameter to be twice the deviations' mean.

We investigated the presence of surround inhibition by stimulating the cells with bright discs of 10 diameters presented in a random order against a dark background. The discs were concentric with the receptive field and flickered 10 times over 12 s (as for the receptive field measurements), and their diameters varied from 75 to 1,200 μm. For each cell, the diameters were equally spaced in a logarithmic scale.

The stimuli used for determining the responses of ganglion cells to motion were bright and dark edges appearing behind circular apertures of 0.7–1.0 mm diam on the retina. The distance between the edges was 1.03 mm so that only one edge appeared in the window at every instant. The edges moved in 16 equally spaced directions (22.5°) and at eight speeds, which were 250, 500, 750, 1,000, 1,250, 1,500, 2,000, and 3,000 μm/ s. The conditions (combinatorial arrangements of directions and speeds) were presented in random order for 12 s each, yielding more passes of edges for higher speeds than for lower ones. This sampling time and the speeds used yielded an integer number of appearances and sweeps of ON and OFF edges. Using an integer number was important to avoid measuring responses to fractions of cycles.

Figure 1*A* illustrates the method used to determine whether a cell was directionally selective for a given speed and to measure the preferred direction. Directional polar plots of the total number of action potentials were constructed for each speed. After the plots' centroids were found, we tested for statistical differences between the centroids and the origin (2-sided *t*-test, $P < 0.01$). If there was a difference, the direction of the vector connecting the origin to the centroid was stored in the computer as the preferred direction.

Figure 1*B* illustrates the method used to determine whether a cell was orientationally selective for a given speed and to measure the preferred orientation. This method, which is similar to that used by Blasdel (1992), first transforms a polar plot with apparent single-axis anisotropy into a polar plot similar to those of directionally selective cells. After this transformation, one can use the same methods as described for directional selectivity. This transformation begins by summing responses to opposite directions, that is, of same orientation. The result of the sum is plotted in a new polar plot at an angle equal to the directions multiplied by 2. As illustrated in the figure, multiplication of opposite directions by 2 always yields the same direction. Furthermore, perpendicular orientations in the original plot are transformed by this procedure into opposite directions. Consequently, orientation selectivity is transformed into pseudodirectionality. After the calculation of the pseudopreferred direction, its value is divided by 2 and added to 90° to obtain the real preferred orientation.

We found that some cells expressed directional or orientation selectivity at several speeds. To know whether a cell displayed true selectivity, it was necessary to test whether the preferred direction or orientation fell within a significantly coherent range.

From the speeds that yielded statistically significant directional selectivity, we calculated the binomial probability (P_D) that their observed range of preferred directions could be accounted for by a distribution where all preferred directions are equally probable. For a range <180° this probability is

$$P_D = n\left(\frac{\theta_D}{360}\right)^{n-1}$$

where n is the number of speeds yielding statistically significant directional selectivity and θ_D is the narrowest angle containing all preferred directions (directional range). The derivation of this equation is as follows: the n randomly sampled directions must all lie within a range smaller than θ_D. Say the nth sample produced the most counterclockwise direction of the group. Then the other $n-1$ must lie clockwise within θ_D of that direction. The probability of this happening is $P_c = (\theta_D/360)^{n-1}$. Because any of the samples might have produced the most counterclockwise direction, the overall probability for a range smaller than θ_D is nP_c, resulting in the equation above. For $\theta_D > 180°$ this equation does not apply, because in this case there are particular configurations of $n-1$ directions lying clockwise within θ_D of a given direction that define a range for which this direction is not the most counterclockwise. A formula to take into account all these configurations can be derived, but is cumbersome. Instead of deriving such formula, we estimated P_D for $\theta_D > 180°$ by computer simulations. In these

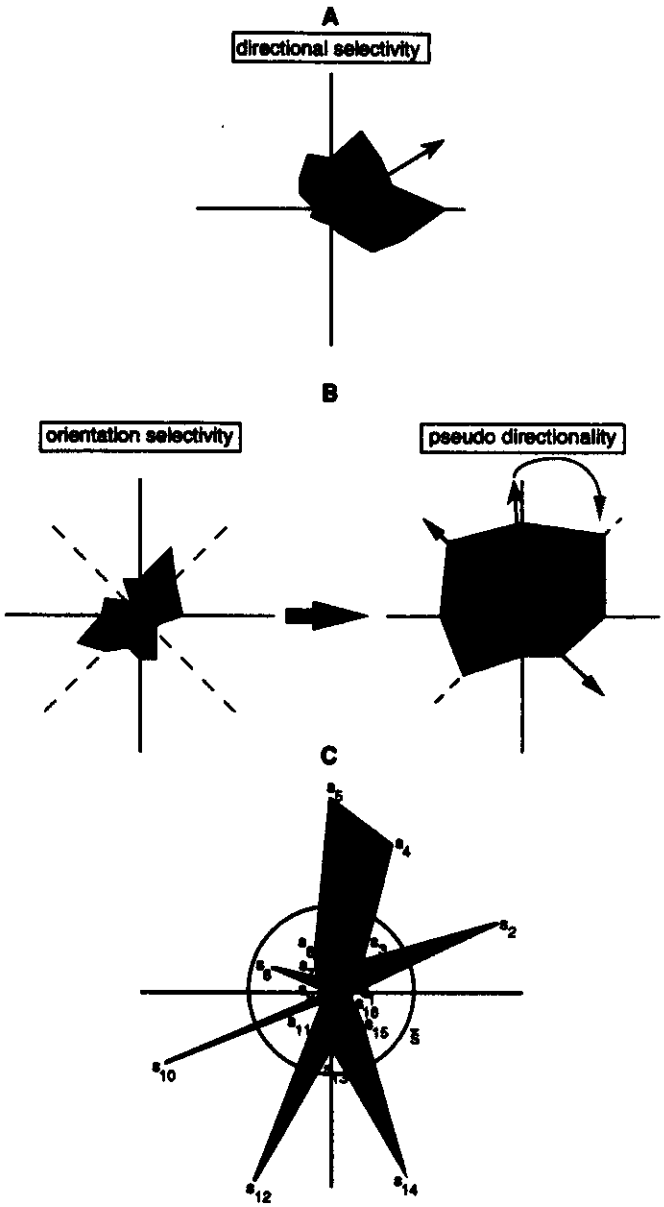

FIG. 1. Methods used to quantify sensitivities to direction and orientation, and the degree of anisotropy. *A*: schematic directional polar plot (shaded area) along with its centroid (•), which is significantly different from the origin, and an arrow from the origin through the centroid. The direction of the arrow is the preferred direction. *B*: procedures used to calculate preferred orientation. *Left panel*: schematic orientational polar plot. Opposite directions are transposed to the same direction and perpendicular orientations to opposite directions. *Right panel*: sum of these transposed responses (which are multiplied by 2), transforming the original orientational plot into a plot with pseudodirectionality. The centroid is used to compute the pseudopreferred direction, which when divided by 2 (stippled arrow) and added to 90° gives the preferred orientation (double arrow line). *C*: how the degree of anisotropy was calculated. The total number of spikes obtained during trials (12 s) at 16 different angles (s_1–s_{16}) is averaged, yielding $\bar{s}$ (circle), and s_1–s_{16} are compared with $\bar{s}$ using a χ^2 test.

simulations, n directions were drawn from a uniform distribution over the circle and their directional range was determined. This was repeated 10,000 times and P_D was set to the fraction of these samples for which $\theta < \theta_D$.

A similar probability was calculated for orientations. For a range <90°, this probability is

$$P_O = n\left(\frac{\theta_O}{180}\right)^{n-1}$$

where n is the number of speeds yielding statistically significant orientation selectivity and θ_O is the narrowest angle containing all preferred orientations (orientational range). The derivation of this equation follows the same rationale as that for directional selectivity. For $\theta_O > 90°$ we used computer simulations similar to those of directional selectivity, except that instead of using the directional range we used the orientational range.

Directional selectivity occurs when the response to motions in a given range of directions is significantly larger than the response to motions in the opposite directions. In turn, orientation selectivity occurs when the sum of the responses to back and forth motions along a given range of axes is significantly larger than the sum of the responses to back and forth motions along the perpendicular axes.

If $P_D < P_O$ and $P_D < 0.2$, then the cell was classified as directionally selective. If $P_O < P_D$ and $P_O < 0.2$, then the cell was classified as orientationally selective. The 0.2 criterion was chosen so that the incidence of directionally selective cells in adults was similar to the level (20–25%) observed in other adult turtle studies (Bowling 1980; Marchiafava 1979). Making the levels comparable was necessary, because our criteria for directional selectivity were more restrictive than those of previous studies because we required the cells to be directionally selective over a broad range of speeds.

Because light responses could be contaminated by spontaneous bursts of activity, these responses might sometimes have been abnormally strong. Such contamination was rare because prolonged exposure of the retina to light during the experimental protocol typically abolished the spontaneous bursts. For the few cases in which they occurred, we removed the abnormal responses by outlier removal procedures. Calculation of P_D and P_O was preceded by outlier removal based on the Dixon test ($\alpha < 0.1$, Dunn and Clark 1987). In this test, the shortest distances (angles) between an outlier candidate and the two extremes of a cluster of preferred directions or orientations were measured. The Dixon test uses the ratio between these distances (shorter distance divided by longer distance), and the outlier is removed if the ratio is too large.

We noticed during the experiments that many immature cells had anisotropic polar plots, responding optimally to several axes of orientation or vectors of direction. Therefore we decided to determine quantitatively the degree of anisotropy in all cells at all developmental stages investigated. For that purpose, we used a χ^2 test (performed using Statview 512+TM on a Macintosh IIsi computer). Our rationale for using this test was to consider the population of spikes as if any given spike has a fixed probability of belonging to 1 of the 16 categories defined by the direction of motion. As such, this population defines a multinomial distribution. Under this assumption we performed a χ^2 test to verify whether our sample came from an homogenous multinomial distribution (Hays 1981). Figure 1*C* illustrates how the values were determined to perform the test. For each cell and at every speed, the total number of spikes obtained at each angle (s_1–s_{16}) were averaged. The value of the average, $\bar{s}$, is represented by the circle in Fig. 1*C*. The χ^2 test determines whether the sum of the deviations from the mean encountered in s_1–s_{16} are significant, and it uses the following equation

$$\chi^2 = \sum_{i=1}^{16} \frac{(s_i - \bar{s})^2}{\bar{s}}$$

Therefore the degree of anisotropy increases with χ^2. For an ideal, hypothetical isotropic cell, that is, a cell whose responses to motion are exactly equal in all directions, $s_i = \bar{s}$ for $i = 1, \ldots, 16$, and thus $\chi^2 = 0$.

The test was repeated for all eight speeds, yielding eight χ^2 values for each cell. The final χ^2 value chosen to characterize the

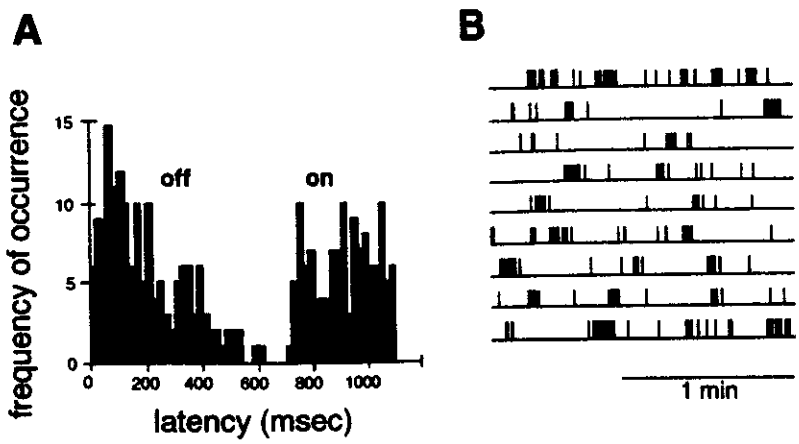

FIG. 2. Light responses and spontaneous bursts of activity. *A*: 1.1-s cumulative poststimulus time histogram of the responses of an embryonic ganglion cell (stage 25) to stationary discs of light concentric with the receptive field, with diameters <1.2 mm and flickering with a 1.2-s period (OFF and ON at 0 and 600 ms, respectively). The OFF response starts within a much shorter delay than the ON response. The ON and OFF responses demonstrate functional synapses from photoreceptors to ganglion cells. *B*: spontaneous bursts of activity from a stage 23 ganglion cell. These bursts were observed from stage 22 until 2–4 wk posthatching.

cell was calculated as the median of all eight values. We determined the probability p (15 degrees of freedom) that a given homogenous multinomial distribution of directions yields a χ^2 value larger or equal to the experimental value. A cell was determined to be anisotropic if $P \leq 0.01$.

RESULTS

We obtained extracellular recordings of light responses from 27 turtle retinas from 35 embryonic ganglion cells (from stage 23 to 26, approximately the last third of gestation), from 44 ganglion cells during the first 40 days posthatching, and from 30 adult ganglion cells. Spontaneous bursts of spikes were recorded from 83 of these cells in 20 embryonic and posthatching retinas. Figure 2*A* illustrates the cumulative poststimulus time histogram obtained from one ON-OFF ganglion cell (stage 25) when exposed to flickering stationary discs of light. We observed ON, OFF, and ON-OFF responses at all stages, suggesting relatively early embryonic establishment of functional synaptic connections from photoreceptors to ganglion cells in both the ON and OFF pathways. Surround inhibition was present at all stages, as evidenced by a bell-shaped dependence of spike counts on disc sizes (see METHODS).

Embryonic cells fired in spontaneously recurring bursts of spikes (Fig. 2*B*). Spontaneous recurring bursts of activity were recorded from stage 22. Similar spontaneous, sensory-independent bursting activity has been observed in mammalian developing retinal ganglion cells (Maffei and Galli-Resta 1990; Masland 1977; Meister et al. 1991; Wong et al. 1993). These spontaneous bursts of activity disappeared within 2–4 wk posthatching.

We investigated responses of developing and adult ganglion cells to edges of light moving in 16 directions and at eight speeds. Figure 3 illustrates the different ways ganglion cells, from embryonic to adult stages, responded to these moving stimuli. Polar plots of these responses, represented in this figure by the total number of spikes pooled across speeds that yielded significant responses, revealed properties well known in adult retinas: directional selectivity (single-axis asymmetry), orientation selectivity (single-axis anisotropy), and isotropic properties. However, polar plots of some immature ganglion cells revealed more complicated features: they exhibited multiple axes of orientation or vectors of direction. We call this property "multiaxis anisotropy." It could be argued that such pooled polar plots do not reflect real and complicated trends in the motion tuning of these cells, but rather result from noise pooled at the eight different speeds. However, Figs. 4 and 5 show that multiaxis anisotropy is a real physiological trend encountered in immature ganglion cells. Figure 4 illustrates the polar plots ob-

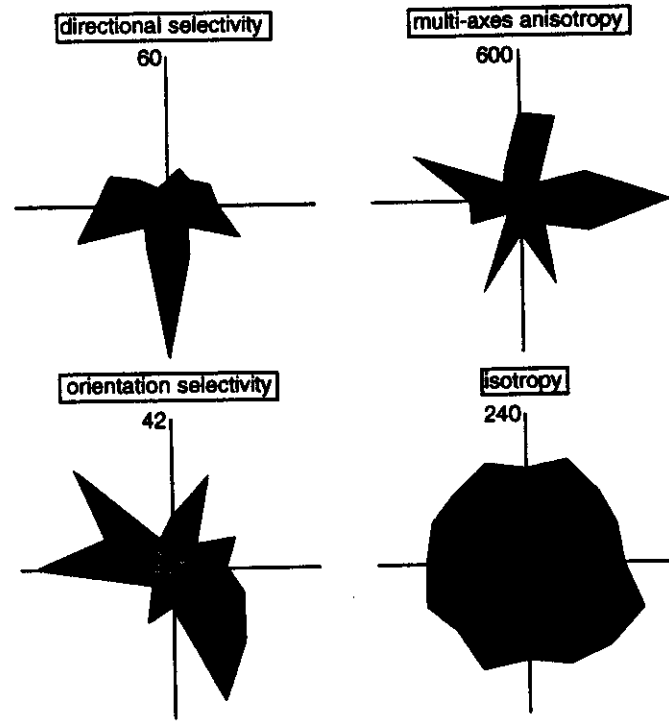

FIG. 3. Four different examples of summed directional polar plots. *Top left panel*: directionally selective adult ganglion cell (at speeds of 750, 1,250, 1,500, and 2,000 μm/s, which were the speeds yielding significant directional selectivity parameters, see METHODS). *Bottom left panel*: orientationally selective stage-23 embryonic cell (at speeds of 1,000, 1,250, 1,500, and 2,000 μm/s, which yielded significant orientation selectivity). *Top right panel*: stage 25 embryonic cell with multiaxis anisotropy. *Bottom right panel*: isotropic cell from a ~14-day-old hatchling. Both plots on the *right panels* were obtained by pooling the responses obtained at all 8 speeds. The distance from the origin in the polar plots is the total number of action potentials for the speeds used (the number on each vertical axis represents the number of action potentials from the origin to the extremity of the axis). The angles in these plots correspond to the directions of motion.

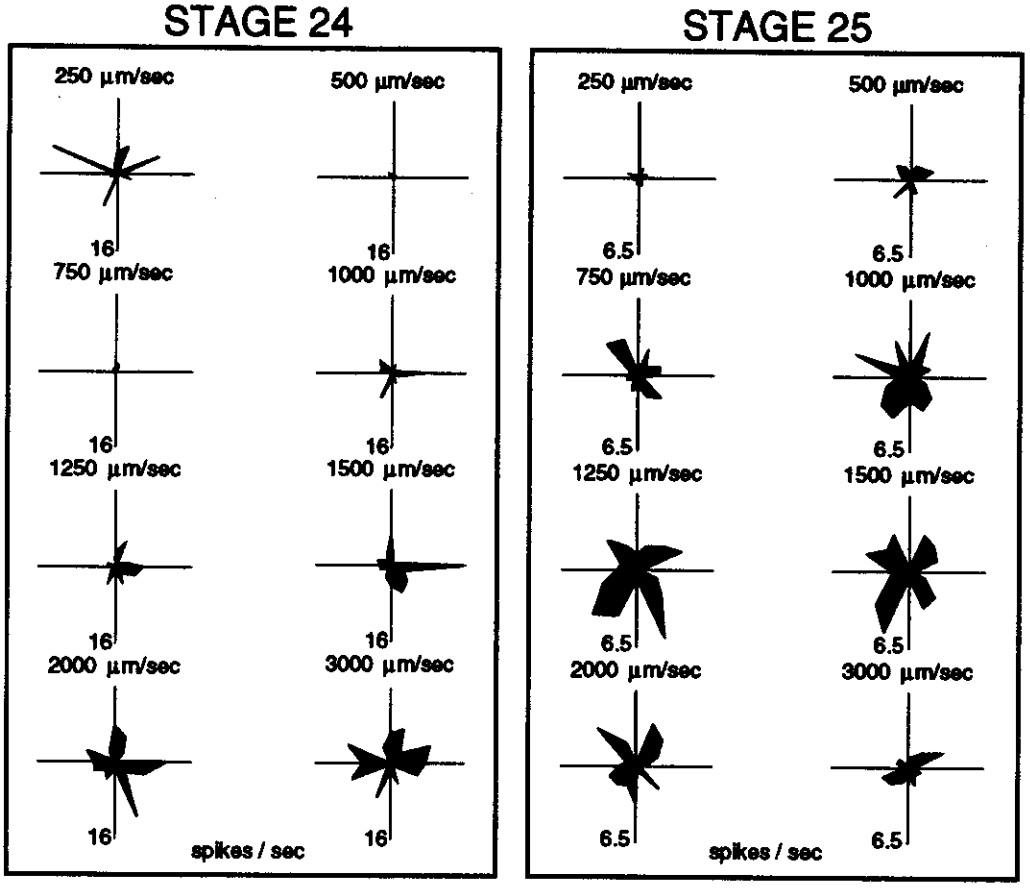

FIG. 4. Embryonic anisotropy is a real physiological trend. This figure shows how 2 embryonic cells (stage 24 and 25 for *left* and *right panel*, respectively) respond to motion at 8 different speeds (polar plot conventions as in Fig. 3). Each panel illustrates the polar plots of the responses (spikes/s) obtained at these speeds. The responses are highly anisotropic, and the pattern of anisotropy (number and orientation of the different lobes) shows some degree of similarity at the different speeds that yield significant responses.

tained separately at each speed for two embryonic cells. It can be seen for each cell that the anisotropic trends (number and orientation of the different lobes) encountered have some degree of similarity at speeds that yielded significant responses. Multiaxis anisotropy was also observed in hatchlings, as is illustrated Fig. 5, *left panel* (this cell was from a 9-day-old hatchling). However, many ganglion cells from hatchlings, but not from embryos, expressed isotropic properties, as shown in Fig. 5, *right panel* (this cell was from a ~14-day-old hatchling). Figures 4 and 5 also illustrate an occasional complex dependence of the responses on speed in immature cells. A strong response was obtained at the lowest speed, then decreased to a minimal value at the next speed and gradually increased toward the fastest speed. We have not yet investigated the reasons for this behavior.

We investigated the time course of maturation of adult receptive field properties of ganglion cells. Figure 6 summarizes the developmental changes in the percentage of directional (black columns) and orientationally selective (gray columns) cells in the recorded sample. Embryonic cells were divided into two age groups, namely stages 23–24 (N = 16) and stages 25–26 (N = 19). Hatchlings were also divided into two age groups, delimited by the end of the 3rd wk posthatching (<3 wk, N = 34; >3 wk, N = 10), which divided the entire sample (from 0 to 40 days posthatching) into two periods of similar duration. Finally, these properties were also investigated in adults (N = 30). Both directional (18% of the entire population) and orientationally selective cells (25%) were already present at stages 23–24, when ganglion cells first started responding to light. The percentage of orientationally selective cells appeared to decrease toward hatching, at stages 25–26. However, it dramatically increased as soon as hatching occurred and remained high during the entire period at which hatchlings were sampled (it was found in 35% of the cells in retinas at <3 wk, and 40% of the cells in retinas at >3 wk). Finally, the incidence of orientationally selective cells dropped to 7% in adults. Directional selectivity, on the other hand, completely disappeared in hatchlings, only to reappear in 20% of the adult cells.

The relatively high incidence of asymmetries and anisotropies (orientation and directional selectivity, and multiaxis anisotropy) and the absence of isotropic cells in embryonic retinas raised the possibility that all spatiotemporal receptive field properties of ganglion cells emerge from initially highly anisotropic embryonic features. Therefore we examined the degree of anisotropy expressed by ganglion cells across development. To quantify this degree of anisotropy we compared the total number of spikes obtained from each cell at each of the 16 angles using a χ^2 test (see METHODS; the

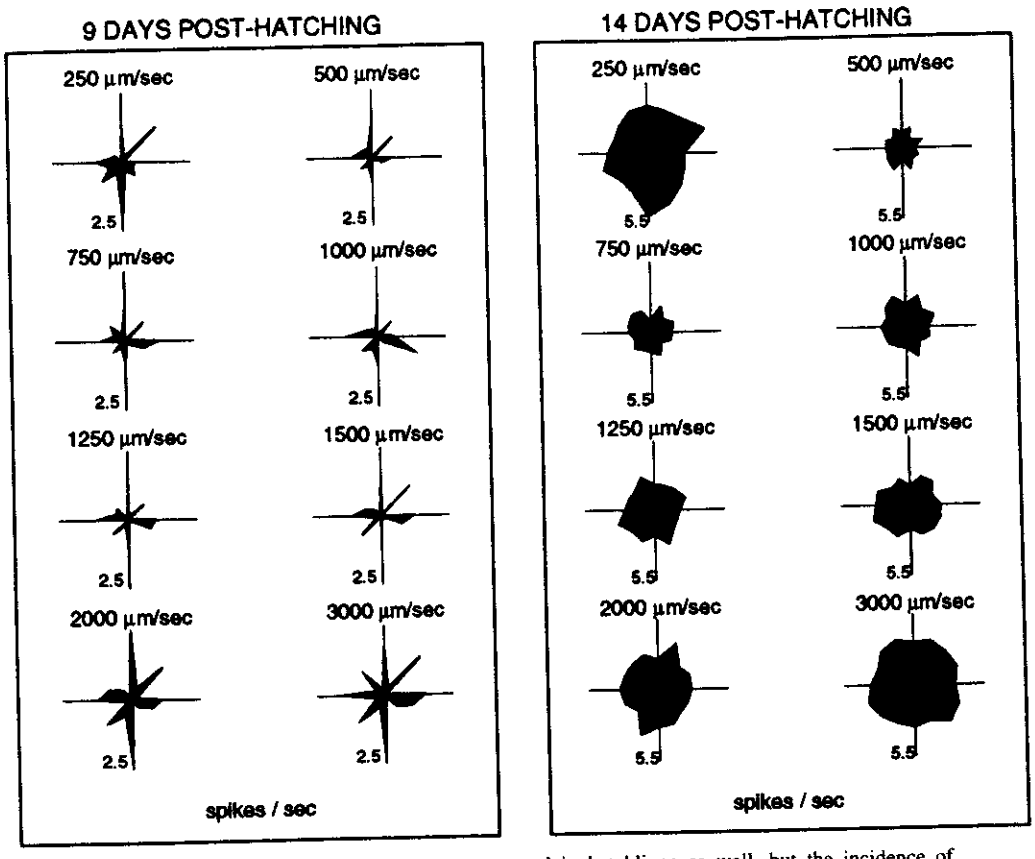

FIG. 5. Anisotropy and isotropy in hatchlings. Anisotropy is encountered in hatchlings as well, but the incidence of anisotropic cells is lower, and many cells start revealing more homogenous isotropic receptive field properties. Responses displayed as in Fig. 4. *Left panel*: responses from a 9-day-old hatchling. These responses are still highly anisotropic and well repeated across different speeds. *Right panel*: isotropic responses from a ~14-day-old hatchling (same cell as in Fig. 3, *bottom right panel*).

degree of anisotropy increases with the value of χ^2). Figure 7 shows that χ^2 values decrease gradually during development. For each stage the individual χ^2 values (which are medians of values obtained at 8 different speeds) obtained from all sampled cells are plotted (◇). The median of each population is plotted as well (●), showing the general decrease in the degree of anisotropy as the retina matures. The dashed line indicates the $P < 0.01$ statistical threshold cho-

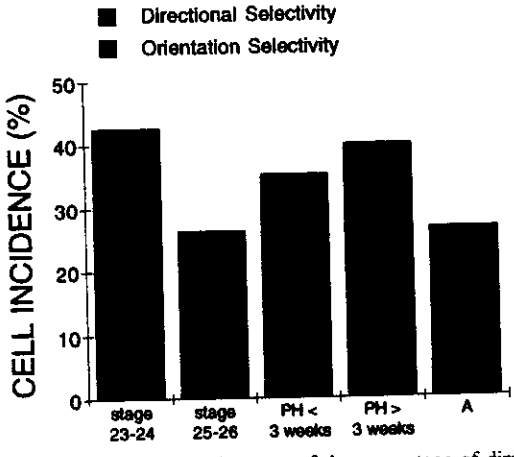

FIG. 6. Time course of development of the percentage of directionally (black columns) and orientationally (gray columns) selective ganglion cells in the entire population sample. Both properties are present from the earliest stages, but directional selectivity disappears in hatchlings to reappear in adults, whereas orientation selectivity peaks in hatchlings. PH, posthatching; A, adults.

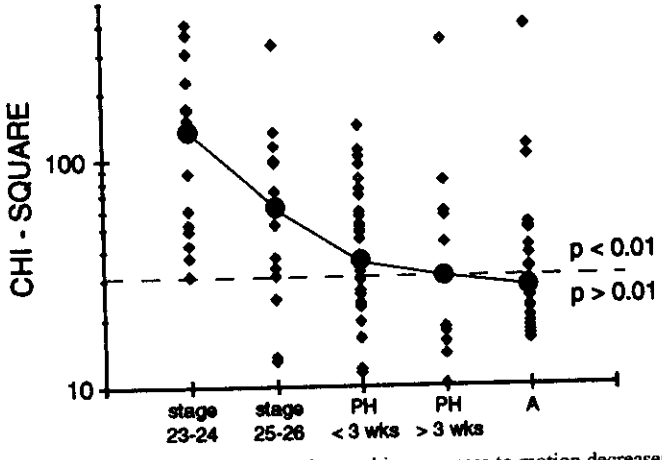

FIG. 7. Degree of anisotropy observed in responses to motion decreases during development. The plot illustrates χ^2 values (see METHODS) for all the cells investigated, grouped according to developmental stages. Values of χ^2 (◇) for each individual cell are plotted on a logarithmic scale for every stage, showing their distribution. The medians (●) of the populations are plotted as well to emphasize the decrease in anisotropy during development. Dashed horizontal line: threshold for statistically significant anisotropy ($\chi^2 = 30.578$, $p = 0.01$, 15 degrees of freedom).

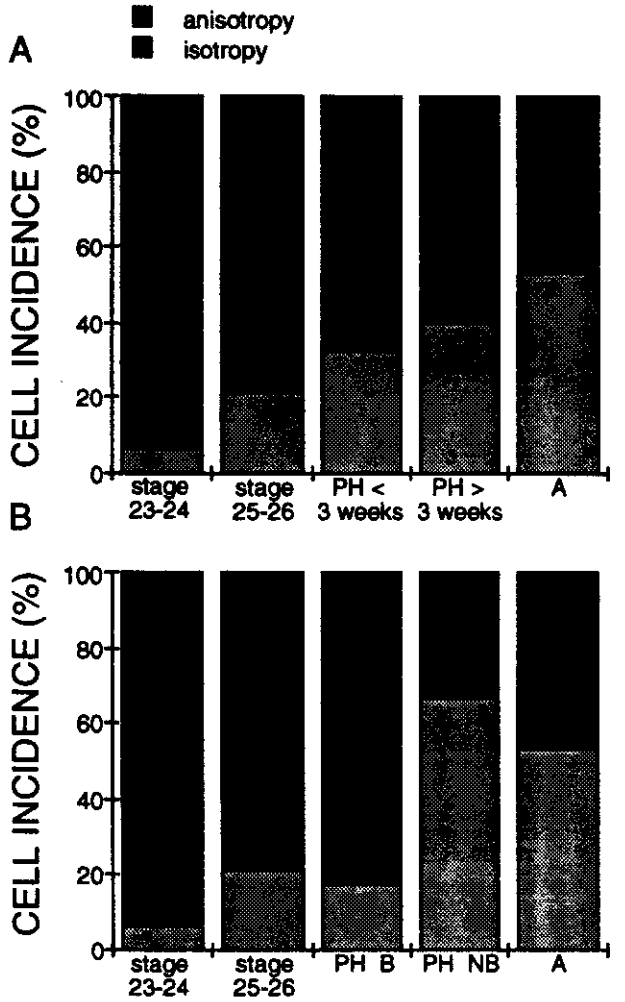

FIG. 8. Percentage of anisotropic cells (black columns) in the sample decreases across development, whereas the percentage of isotropic cells (gray columns) increases. Moreover, stabilization of isotropy coincides with the disappearance of the spontaneous bursts of activity, 2–4 wk posthatching, suggesting a role for spontaneous activity in the development of isotropic receptive field properties of ganglion cells. The percentage of isotropy was calculated from cells that were neither directionally nor orientationally selective and that had a probability >0.01 in the χ^2 test. *A*: how isotropy increases and anisotropy decreases chronologically during development. *B*: same plot as in *A*, except for the classification of cells in hatchlings. They were classified according to whether they were still expressing spontaneous bursts of spikes. The incidence of isotropy stabilizes at the same time the spontaneous bursts disappear, regardless of the absolute age of the retina. PH B, posthatching with bursts; PH NB, posthatching with no bursts.

sen for significant anisotropy. At stages 23–24 all cells were anisotropic. The incidence of anisotropic cells then decreased to reach a minimum in adults. This strongly suggests that mature receptive field properties of ganglion cells emerge from initially highly anisotropic embryonic properties. Figure 8*A* shows the time course of development of isotropy (gray columns). The incidence of isotropy was calculated from cells that were neither directionally nor orientationally selective and had a probability >0.01 in the χ^2 test. Anisotropy (black columns) includes directional and orientation selectivity as well as cases in which $P < 0.01$ in the χ^2 test. The incidence of pure isotropy, according to our criteria, increased with development and reached a maximum in adults.

Spontaneous bursts of spikes were present in all embryonic ganglion cells and disappeared 2–4 wk posthatching, during a period when the incidence of isotropic and anisotropic cells approached maturation. Therefore we looked for a possible temporal correlation between the disappearance of the spontaneous bursts and stabilization of isotropy-anisotropy to mature levels. Figure 8*B* illustrates the time course of development of isotropy-anisotropy, as in Fig. 8*A*, with the only difference being that hatchling populations were classified according to the presence or absence of spontaneous bursts instead of the absolute age of the cells. The stabilization in incidence of isotropic cells once the spontaneous bursts disappear suggests a role for ganglion cell spontaneous activity in shaping concentric (isotropic) receptive fields. The large increase in incidence from bursting to nonbursting conditions in Fig. 8*B* is not due to random bursting causing an impression of anisotropy. Evidence against this possibility comes from the similarity of polar plots across speeds in Figs. 4 and 5. Moreover, when embryonic cells were stimulated with an edge of light moving at eight speeds but only in 1 instead of 16 directions, anisotropic patterns were not observed and the responses were statistically isotropic. Figure 9 compares the χ^2 values obtained from such controls obtained in five stage 25 ganglion cells with the sample of ganglion cells of similar age taken from Fig. 7. Although these control cells were spontaneously bursting like cells in the other sample, the control χ^2 values were lower than their counterpart, indicating that such intrinsic noise (perhaps reflected in the distribution of χ^2 values) cannot account for the level of anisotropy observed in embryonic cells.

Receptive field properties observed during development may reflect the maturation of dendritic trees of ganglion and/or other cells in the retina. Therefore we looked at changes in receptive field sizes during development (Fig. 10). Receptive fields expanded rapidly posthatching, reaching adult

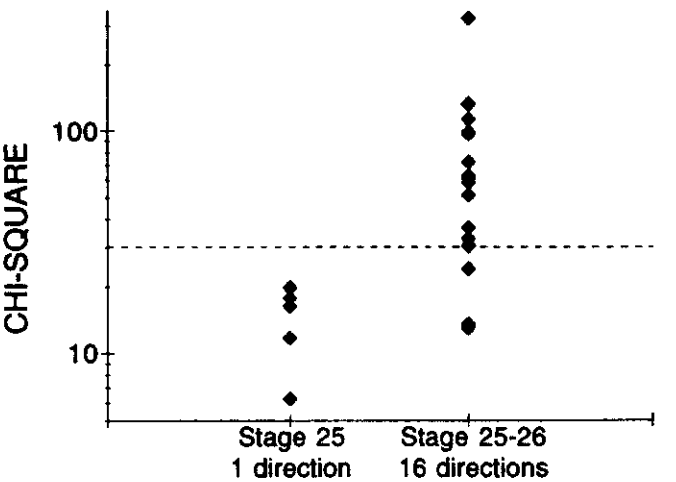

FIG. 9. Intrinsic noise in spontaneously bursting embryonic ganglion cells does not account for the presence of embryonic anisotropy. The plot illustrates χ^2 values as in Fig. 7. The population of values on the *right side* of the graph was taken from Fig. 7. The χ^2 values on the *left side* of the graph were obtained from cells of similar ages and bursting capabilities, and in the same experimental conditions, except that the edge of light never changed direction during the experiment (for each speed the edge was presented in 16 trials of 12 s each). Dashed line as in Fig. 7.

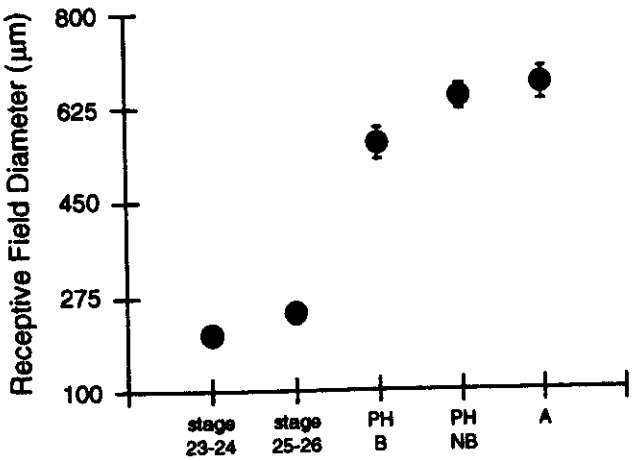

FIG. 10. Development of receptive field size. The results suggest that excitatory receptive field sizes reach maturity as spontaneous bursts disappear. Furthermore, a >2-fold receptive field expansion during the 1st mo posthatching suggests an expansive role for light-evoked activity. Data are mean diameters over all cells as function of age with standard error bars. The visual streak could not be seen at embryonic and posthatching stages, but receptive fields were sampled from the central part of the retina. Adult receptive fields were sampled within or as close as possible to the visual streak.

sizes in hatchlings. The receptive field size maturation coincided with the disappearance of spontaneous burst activity (there was a significant difference between the diameter of receptive fields in hatchlings with bursts and without bursts: 2-sided t-test, $p < 0.05$, 67 degrees of freedom) and thus with stabilization of the incidence of concentric ganglion cells (see Fig. 8).

In adult retinas, receptive field sizes can correlate well with the sizes of the dendritic trees (Amthor et al. 1989; Bloomfield 1994; Criswell 1987; Yang and Masland 1992). Such parallelism between dendritic topography and receptive field properties may not be readily detectable in our embryonic receptive field mapping because immature dendrites might be shorter than 100 mm, the size of our mapping spot. We tested smaller spots (30–60 mm), but unfortunately they did not elicit firing. However, we could sometimes observe a parallelism between the spatial organization of the receptive field and the occurence of orientation selectivity in hatchlings. For example, Fig. 11 illustrates the elongated receptive field from an orientationally selective ganglion cell in a 14-day-old retina. The preferred orientation of that cell was −6°, a parallel match with the longest axis of the receptive field.

DISCUSSION

The results of this study show that embryonic retinal ganglion cells in the turtle not only fire in spontaneous bursts of action potentials but also respond to light. Early embryonic ganglion cells are highly anisotropic, showing a wide variety of complicated patterns of multiaxis anisotropy. From the earliest stages in ontogeny, when ganglion cells start responding to light, until several weeks after hatching, the shape of these spatiotemporal receptive fields is modified and becomes gradually simpler, being replaced by concentric (isotropic) receptive fields. The incidence of isotropic ganglion cells stabilizes at the same time as the spontaneous bursts disappear, and thus shows temporal correlation with the maturation of excitatory receptive field sizes, at 2–4 wk posthatching. Both directional and orientation selectivity are present from the earliest embryonic stages. But sensitivity to direction completely vanishes once the retina is exposed to light, only to reappear in adults. In contrast, orientation selectivity reaches its highest incidence in hatchlings and then decreases in adults.

One important conclusion from this study is that mature spatiotemporal receptive field properties arise from highly anisotropic properties expressed by ganglion cells during embryogenesis. This embryonic behavior does not result from noise or cell fatigue, because our results clearly indicate that the pattern of anisotropy observed for each individual cell is relatively well repeated for trials performed at different speeds, and such anisotropic patterns are not expressed when the light edge moves all the time in the same direction. Moreover, despite using a χ^2 test to measure the degree of anisotropy and thus giving a better chance of passing the test to cells that have a high firing rate, we found that χ^2 values were highest in the youngest cells (which often have a low firing rate) and then gradually decreased. Taking into account this bias due to the χ^2 test, the decrease in degree

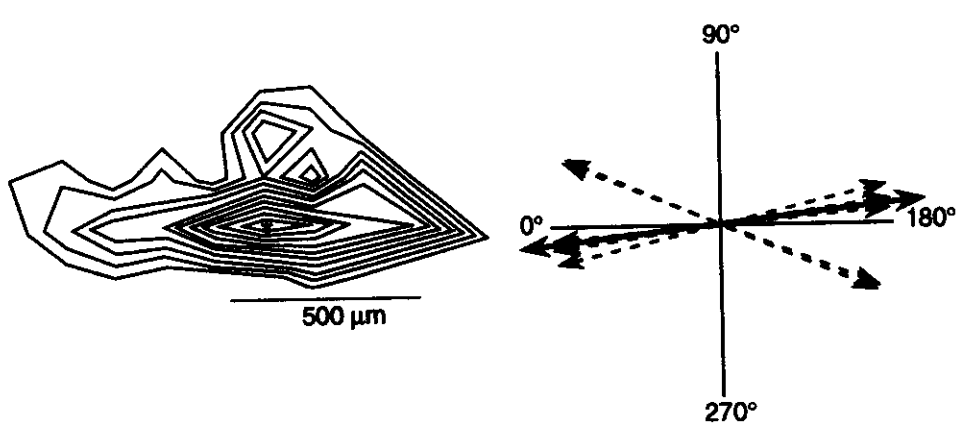

FIG. 11. Some orientationally selective ganglion cells have elongated receptive field areas. This figure illustrates the receptive field topographic map (*left panel*) obtained from a 14-day-old ganglion cell that was orientation selective (preferred orientation −6°; $P < 0.01$; 2-sided t-test). Concentric lines: areas of similar light-driven firing rate. Asterisk: area in the field with the highest firing rate (11 spikes/s). From the center toward the periphery, each line indicates an additional 1-spike/s drop in firing rate. *Right panel*: statistically significant preferred orientations of that cell obtained at 6 speeds (dashed double-headed arrows) and the preferred orientation (solid double-headed arrow), which was −6°, the median of the 6 values. Both panels are oriented the same way: 0–180° left to right, and 90–270° up to down.

of anisotropy across development may be even steeper than revealed by our data.

Because the timing of maturation of receptive field dimensions shows a correlation with the maturation of isotropic cells and a decrease in anisotropy, we propose that embryonic anisotropy reflects immature, polarized, and poorly branched dendritic trees. As dendrites elongate and branch, they loose their polarity and cover a more homogenous field, and thus the cells become isotropic. This idea is reinforced by anatomic studies of developing ganglion cells in mammals (Dunlop 1990; Maslim et al. 1986; Ramoa et al. 1988) and avians (Vanselow et al. 1990) showing that immature ganglion cells have small and polarized dendritic trees that expand and branch with maturation. Such a possible parallelism between the dendritic layout of turtle ganglion cells and their receptive field properties remains to be determined and is under investigation in our laboratory.

Both directional and orientation selectivity are present early in ontogeny. Single-axis dendritic tree polarization throughout life (Bloomfield 1991, 1994), or strengthening of synaptic connections related to early embryonic polarization, may be the reason for the presence of orientationally selective cells at all stages. We also found that six orientationally selective ganglion cells in hatchlings (when this property is predominant) had clearly elongated receptive fields (as in Fig. 11). In five of these cells the fields were elongated in the preferred orientation, and in one cell the field was perpendicular to the preferred orientation. Embryonic directional selectivity completely disappears at hatching, only to reappear in adults (we do not know at this point when it reappears). When embryonic and adult parameters of directional selectivity were compared, no significant difference was observed either in the number of speeds yielding directional selectivity (3.6 ± 0.6 speeds, mean $\pm$ SE, for adults, $N = 7$; 2.8 ± 0.5 speeds for embryos, $N = 6$) or in the statistical strength of that property ($P_D = 0.08 \pm 0.02$ for adults and 0.06 ± 0.02 for embryos). However, we will need larger samples of directionally selective cells to make a solid statistical statement about possible differences. Nevertheless, the fact that directional selectivity disappears to reappear only much later during development suggests that embryonic and adult directional selectivity do not necessarily share common mechanisms. Embryonic directional selectivity may be accidental and result from dendritic cable properties, e.g., delayed voltage propagation of embryonic synaptic potentials along dendrites in polarized dendritic trees (Borg-Graham and Grzywacz 1992; Rall 1964). This could occur either in the ganglion cell itself, with signals propagating toward the soma, or in amacrine dendrites making synaptic contacts on the ganglion cell, with signals propagating toward the dendritic ending. Moreover, it is very likely that synaptic responses are weaker in embryos than in hatchlings and adults. Such weak signals could result not only in delay but sometimes even in failure of transmitter release from amacrine dendrites or generation of action potentials in ganglion cells. While ganglion cells grow and their responses become more robust, embryonic directional selectivity disappears. Biophysical models of embryonic directional selectivity generated by dendritic cable properties are currently under investigation in our laboratory (Grzywacz and Sernagor 1994). Retinal ganglion cell death could also account for the presence of embryonic directional selectivity. It is known that ganglion cell survival depends on ganglion cell dendritic competition for establishment of synaptic connections (Perry and Linden 1982). In the turtle retina, ganglion cells go through a period of cell death from stage 22–25 (Sernagor, unpublished data). These dying cells perhaps have weaker synaptic responses, and therefore may be more prone to accidental directional selectivity, as proposed above.

Changes in morphological outline of the dendritic tree do not seem to explain the late emergence of mature directional selectivity. The increase in dimensions of dendritic trees and their degree of polarization do not appear to account for the development of directional selectivity because, when the size of receptive fields and the incidence of isotropic cells reach maturity in hatchlings, mature directional selectivity is still absent. Therefore we suggest that the expression of directional selectivity requires either light exposure (visual experience) or the late establishment of a specialized inhibitory synaptic drive onto part of the network mediating orientation selectivity in ganglion cells. Directional selectivity must emerge at the expense of other receptive field properties, and the percentage of orientationally selective cells, but not of isotropic cells, decreases dramatically from hatchlings to adults. Thus it is reasonable to suggest that directional selectivity builds on orientation axes or, in other words, mature directionally selective ganglion cells are modified orientationally selective cells.

The timing of maturation of concentric cells coincides with the disappearance of the spontaneous bursts and thus correlates with the timing of maturation of the excitatory receptive field size. We suggest that these spontaneous immature bursts of activity in ganglion cells may play an important role in dendritic outgrowth (in accordance with a study by Wong et al. 1991) and that they contribute to the establishment of isotropic receptive field properties in developing ganglion cells. However, these spontaneous bursts do not seem to play a direct role in the emergence of directional selectivity, because this property emerges after the spontaneous bursts disappear. [In rabbits, directional selectivity also matures late relative to the disappearance of the spontaneous bursts (Masland 1977), although the development of the rabbit retina spans a shorter period than that of the turtle.]

As soon as turtles hatch there is a dramatic increase in the size of excitatory receptive fields (but not of the eyes), and within 2–4 wk the incidence of concentric fields stabilizes to mature levels and the spontaneous bursts vanish. These findings lead us to think that visual experience is important in completing processes that have started in embryonic retinas that are essentially deprived of sensory inputs. Moreover, recent findings obtained from dark-reared hatchlings (Sernagor and Grzywacz 1994) strongly suggest that embryonic spontaneous bursts and visual experience may play complementary roles: spontaneous activity may induce and constantly stimulate dendritic outgrowth in developing ganglion cells, whereas exposure to light first accelerates and then terminates these processes. We found that within the 1st mo posthatching (we did not investigate beyond that point), light-deprived ganglion cells remain spontaneously active, whereas their excitatory receptive fields become larger, less isotropic, and with less orientation selectivity, than in normal hatchlings.

We thank Drs. David Peterzell and Ehud Zohary for helpful suggestions about the presentation of the results. and Drs. Lyle Borg-Graham, Nigel Daw, Takuji Kasamatsu, Manfred Mackeben, Michael O'Donovan, and Harvey Smallman for critical reading of the manuscript. We also thank H. and M. Kliebert for supplying the turtle eggs.

Support for this work came from National Eye Institute Grant EY-08921 and Office of Naval Research Grant N00014-91-J-1280, from an award from the Paul L. and Phyllis C. Wattis Foundation, and from core Grant EY-06883 to Smith-Kettlewell.

Address reprint requests to E. Sernagor.

Received 6 July 1994; accepted in final form 29 November 1994.

REFERENCES

AMTHOR, F. R. AND GRZYWACZ, N. M. Directional selectivity in vertebrate retinal ganglion cells. In: *Visual Motion and its Role in the Stabilization of Gaze*, edited by F. A. Miles and J. Wallman. Amsterdam: Elsevier, 1993, p. 79–100.

AMTHOR, F. R., TAKAHASHI, E. S., AND OYSTER, C. W. Morphologies of rabbit retinal ganglion cells with complex receptive-fields. *J. Comp. Neurol.* 280: 97–121, 1989.

BLASDEL, G. G. Orientation selectivity, preference, and continuity in monkey striate cortex. *J. Neurosci.* 12: 3139–3161, 1992.

BLOOMFIELD, S. A. Two types of orientation-sensitive responses of amacrine cells in the mammalian retina. *Nature Lond.* 350: 347–350, 1991.

BLOOMFIELD, S. A. Orientation-sensitive amacrine and ganglion cells in the rabbit retina. *J. Neurophysiol.* 71: 1672–1691, 1994.

BORG-GRAHAM, L. AND GRZYWACZ, N. M. An isolated turtle retina preparation allowing direct approach to ganglion cells and photoreceptors, and transmitted light microscopy (Abstract). *Invest. Ophthalmol. Vis. Sci.* 31: 1039, 1990.

BORG-GRAHAM, L. AND GRZYWACZ, N. M. A model of the direction selectivity circuit in the retina: transformations by neurons singly and in concert. In: *Single Neuron Computation*, edited by T. McKenna, J. Davis, and S. Zornetzer. Orlando, FL: Academic, 1992, p. 347–375.

BOWLING, D. B. Light responses of ganglion cells in the retina of the turtle. *J. Physiol. Lond.* 329: 173–196, 1980.

CRISWELL, M. H. *Cellular Mechanisms of Movement Detection and Directionality in the Turtle Retina* (PhD thesis). Indiana University, program in Physiological Optics, 1987.

DACHEUX, R. F. AND MILLER, R. F. An intracellular electrophysiological study of the ontogeny of functional synapses in the rabbit retina. I. Receptors, horizontal and bipolar cells. *J. Comp. Neurol.* 198: 307–326, 1981a.

DACHEUX, R. F. AND MILLER, R. F. An intracellular electrophysiological study of the ontogeny of functional synapses in the rabbit retina. II. Amacrine cells. *J. Comp. Neurol.* 198: 327–334, 1981b.

DAW, N. W. AND WYATT, H. J. Raising rabbits in a moving visual environment: an attempt to modify direction sensitivity in the retina. *J. Physiol. Lond.* 240: 309–330, 1974.

DUNLOP, S. A. Early development of retinal ganglion cell dendrites in the marsupial *setonix brachyurus*, quokka. *J. Comp. Neurol.* 293: 425–447, 1990.

DUNN, O. J. AND CLARK, V. A. *Applied Statistics: Analysis of Variance and Regression*. New York: Wiley, 1987.

GRZYWACZ, N. M. AND SERNAGOR, E. Development of directional selectivity in turtle retina: physiology and model. *Soc. Neurosci. Abstr.* 20: 1470, 1994.

GRZYWACZ, N. M., SERNAGOR, E., AND AMTHOR, F. R. Retinal directional selectivity: function, mechanism and development. In: *Handbook of Brain Theory and Neural Networks*, edited by M. A. Arbib. Cambridge, MA: MIT Press. In press.

HAYS, W. L. *Statistics*. New York: Holt, Rinehart, & Winston, 1981.

LOHMANN, K. J. How sea turtles navigate. *Sci. Am.* January 266: 82–88, 1992.

MAFFEI, L. AND GALLI-RESTA, L. Correlation in the discharges of neighboring rat retinal ganglion cells during prenatal life. *Proc. Natl. Acad. Sci. USA* 87: 2861–2864, 1990.

MARCHIAFAVA, P. L. The responses of retinal ganglion cells to stationary and moving visual stimuli. *Vision Res.* 19: 1203–1211, 1979.

MASLAND, R. H. Maturation of function in the developing rabbit retina. *J. Comp. Neurol.* 175: 275–286, 1977.

MASLIM, J., WEBSTER, M., AND STONE, J. Stages in the structural differentiation of retinal ganglion cells. *J. Comp. Neurol.* 254: 382–402, 1986.

MATURANA, H. R., LETTVIN, J. Y., MCCULLOCH, W. S., AND PITTS, W. H. Anatomy and physiology of vision in the frog (*rana pipiens*). *J. Gen. Physiol.* 43: 129–171, 1960.

MEISTER, M., WONG, R. O. L., BAYLOR, D. A., AND SHATZ, C. J. Synchronous bursts of action potentials in ganglion cells of the developing mammalian retina. *Science Wash. DC* 252: 939–943, 1991.

PERRY, V. H. AND LINDEN, R. Evidence for dendritic competition in the developing retina. *Nature Lond.* 297: 683–685, 1982.

RALL, W. Theoretical significance of dendritic tree for input-output relation. In: *Neural Theory and Modeling*, edited by R. F. Reiss. Stanford, CA: Stanford Univ. Press, 1964, p. 73–97.

RAMOA, A. S., CAMPBELL, G., AND SHATZ, C. J. Dendritic growth and remodeling of cat retinal ganglion cells during fetal and postnatal development. *J. Neurosci.* 8: 4239–4261, 1988.

SERNAGOR, E. AND GRZYWACZ, N. M. Emergence of isotropic and anisotropic receptive-field properties in turtle developing retina. *Soc. Neurosci. Abstr.* 19: 52, 1993.

SERNAGOR, E. AND GRZYWACZ, N. M. Role of early spontaneous activity and visual experience in shaping complex receptive field properties of ganglion cells in the developing retina. *Soc. Neurosci. Abstr.* 20: 1470, 1994.

VANSELOW, J., DÜTTING, D., AND THANOS, S. Target dependence of chick retinal ganglion cells during embryogenesis: cell survival and dendritic development. *J. Comp. Neurol.* 295: 235–247, 1990.

WONG, R. O. L., HERRMANN, K., AND SHATZ, C. J. Remodeling of retinal ganglion cell dendrites in the absence of action potential activity. *J. Neurobiol.* 22: 685–697, 1991.

WONG, R. O. L., MEISTER, M., AND SHATZ, C. J. Transient period of correlated bursting activity during development of the mammalian retina. *Neuron* 11: 923–938, 1993.

YANG, G. AND MASLAND, R. H. Direct visualization of the dendritic and receptive fields of directionally selective retinal ganglion cells. *Science Wash. DC* 258: 1949–1952, 1992.

YNTEMA, C. L. A series of stages in the embryonic development of *chelydra serpentina*. *J. Morphol.* 125: 219–252, 1968.